

# Observation of phase noise reduction in photonically synthesized sub-THz signals using a passively mode-locked laser diode and highly selective optical filtering

A. R. Criado,<sup>1,\*</sup> P. Acedo,<sup>1</sup> G. Carpintero,<sup>1</sup> C. de Dios,<sup>1</sup> and K. Yvind<sup>2</sup>

<sup>1</sup>Electronics Technology Department, Universidad Carlos III de Madrid, Butarque 15, Leganés, Madrid 28911, Spain

<sup>2</sup>DTU Fotonik, Department of Photonics Engineering, Technical University of Denmark, Ørstedes Plads 343, 2800-Kgs. Lyngby, Denmark  
[acriado@ing.uc3m.es](mailto:acriado@ing.uc3m.es)

**Abstract:** A Continuous Wave (CW) sub-THz photonic synthesis setup based on a single Passively Mode-Locked Laser Diode (PMLLD) acting as a monolithic Optical Frequency Comb Generator (OFCG) and highly selective optical filtering has been implemented to evaluate the phase noise performance of the generated sub-THz signals. The analysis of the synthesized sub-THz signals up to 120 GHz gives as a result an effective reduction of the electrical linewidth when compared to direct harmonic generation that begins at 50 GHz and becomes greater as the frequency increases. The phase noise reduction offered by the setup, along with its integration potential, cost and bandwidth, make it a promising candidate to the development of an integrated and high performance low phase noise local oscillator in the sub-THz range.

©2012 Optical Society of America

**OCIS codes:** (140.4050) Mode-locked lasers; (190.2620) Harmonic generation and mixing; (250.5960) Semiconductor lasers; (350.4010) Microwaves.

---

## References and links

1. P. H. Siegel, "Terahertz technology," *IEEE Trans. Microwave Theory Tech.* **50**(3), 910–928 (2002).
2. C. Jansen, S. Wietzke, O. Peters, M. Scheller, N. Vieweg, M. Salhi, N. Krumbholz, C. Jördens, T. Hochrein, and M. Koch, "Terahertz imaging: applications and perspectives," *Appl. Opt.* **49**(19), E48–E57 (2010).
3. J. Capmany and D. Novak, "Microwave photonics combines two worlds," *Nat. Photonics* **1**(6), 319–330 (2007).
4. S. Ristic, A. Bhardwaj, M. Rodwell, L. Coldren, and L. Johansson, "An Optical Phase-Locked Loop Photonic Integrated Circuit," *J. Lightwave Technol.* **28**, 526–538 (2009).
5. X. Leijtens, "JePPIX: the platform for Indium Phosphide-based photonics," *IET Optoelectron.* **5**(5), 202–206 (2011).
6. H.-J. Song, N. Shimizu, T. Furuta, K. Suizu, H. Ito, and T. Nagatsuma, "Broadband-Frequency-Tunable Sub-Terahertz Wave Generation Using an Optical Comb, AWGs, Optical Switches, and a Uni-Travelling Carrier Photodiode for Spectroscopic Applications," *J. Lightwave Technol.* **26**(15), 2521–2530 (2008).
7. H. Ito, T. Furuta, F. Nakajima, K. Yoshino, and T. Ishibashi, "Photonic generation of continuous THz wave using uni-travelling-carrier photodiode," *J. Lightwave Technol.* **23**(12), 4016–4021 (2005).
8. P. Acedo, H. Lamela, S. Garidel, C. Roda, J. P. Vilcot, G. Carpintero, I. H. White, K. A. Williams, M. Thompson, W. Li, M. Pessa, M. Dumitrescu, and S. Hansmann, "Spectral characterisation of monolithic modelocked lasers for mm-wave generation and signal processing," *Electron. Lett.* **42**(16), 928–929 (2006).
9. P. Acedo, G. Carpintero, A. R. Criado, and K. Yvind, "Photonic Synthesis of sub-THz Signals Using Mode-Locked Single QW Lasers and Tunable Fabry-Perot Fiber Filters," in *European Microwave Week EuMIC11-4*, Paris, France (2011).
10. P. Vasil'ev, *Ultrafast Diode Lasers: Fundamentals and Applications* (Artech House Publishers, 1995).
11. K. Yvind, D. Larsson, L. J. Christiansen, J. Mork, J. M. Hvam, and J. Hanberg, "High-performance 10 GHz all-active monolithic modelocked semiconductor lasers," *Electron. Lett.* **40**(12), 735–737 (2004).
12. G. Carpintero, M. G. Thompson, R. V. Penty, and I. H. White, "Low Noise Performance of Passively Mode-Locked 10-GHz Quantum-Dot Laser Diode," *IEEE Photon. Technol. Lett.* **21**(6), 389–391 (2009).
13. D. Linde, "Characterization of the noise in continuously operating mode-locked lasers," *Appl. Phys. B* **39**(4), 201–217 (1986).

14. D. Eliyahu, R. A. Salvatore, and A. Yariv, "Effect of noise on the power spectrum of passively mode-locked lasers," *J. Opt. Soc. Am. B* **14**(1), 167–174 (1997).
  15. E. Rouvalis, C. C. Renaud, D. G. Moodie, M. J. Robertson, and A. J. Seeds, "Traveling-wave Uni-Traveling Carrier photodiodes for continuous wave THz generation," *Opt. Express* **18**(11), 11105–11110 (2010).
  16. E. Sooudi, G. Huyet, J. G. McInerney, F. Lelarge, K. Merghem, R. Rosales, A. Martinez, A. Ramdane, and S. P. Hegarty, "Injection-Locking Properties of InAs/InP-Based Mode-Locked Quantum-Dash Lasers at 21 GHz," *IEEE Photon. Technol. Lett.* **23**(20), 1544–1546 (2011).
  17. S. Gee, F. Quinlan, S. Ozharar, and P. Delfyett, "Two-mode beat phase noise of actively modelocked lasers," *Opt. Express* **13**(11), 3977–3982 (2005).
- 

## 1. Introduction

Today, the pursue for integrated and cost-effective generation and detection technologies that could allow a widespread access to the potential applications in the sub-THz and THz frequencies has become one of the most active fields of research [1, 2]. A narrow linewidth of the sub-THz signals, in addition to cost and compactness of the proposed solutions, is needed for some of the applications, such as high resolution spectroscopy [2] or broad bandwidth communications [3]; but especially towards the development of heterodyne receivers in this frequency band, where a good quality Local Oscillator (LO) signal is mandatory.

Signal generation by downconversion from the optical domain appears as a promising technology for filling the THz gap mainly because of its integration potential [4, 5] and its good performance [6]. The photonic generation of sub-THz Continuous Wave (CW) signals is carried out by beating in a photomixing device two optical frequencies with a frequency difference equal to that of the electrical signal to be generated. These two optical frequencies can be obtained from two independent lasers, requiring external Optical Phase Locked Loops (OPLL), but providing continuous tunability [7]; or from a single source, like dual-mode devices [8] or Optical Frequency Comb Generators (OFCG), which usually requires additional components as phase modulators or external RF references and offers discrete tunability [6].

In this paper, a compact setup for CW sub-THz photonic synthesis using an OFCG and highly selective optical filtering [9] is employed to study the phase noise performance of the signals synthesized with this scheme and to compare them with those obtained by direct harmonic generation. In this setup, two optical modes are filtered from a Passively Mode-Locked Laser Diode (PMLLD), which is employed as OFCG, and then mixed in a fast photodiode to generate an electrical signal with a frequency equal to the frequency spacing between the two optical modes selected.

Photonic synthesis of electrical signals up to 120 GHz has been accomplished. The analysis of the phase performance of these signals when compare to direct harmonic generation gives as a result an electrical linewidth reduction that becomes more remarkable as the frequency increases. No reduction seems to exist at lower frequencies (less than 50 GHz), but a narrowing in the electrical linewidth begins to appear for frequencies greater than 50 GHz. From this point onwards, the reduction increases as the frequency gets higher, reaching narrowing values of 35% at 110 GHz and 25% at 120 GHz with respect to direct harmonic generation. The reported phase noise improvement of CW sub-THz signals synthesized with this setup along with its integration potential, cost and bandwidth capabilities make it a promising candidate to the development of an integrated and high performance local oscillator in the sub-THz range.

## 2. Mode-locked laser diode as optical frequency comb generator

A mode-locked laser diode (MLLD) is a source of short optical pulses in the picosecond or subpicosecond range. As a semiconductor device, is compact and can be fully integrated on an InP substrate with a central wavelength in the 1550 nm range, that makes it fully compatible with fiber Commercially available Off-The-Shelf (COTS) telecom components. In addition, Photonic Integrated Circuits (PIC) are available to extend integrability to monolithic integrated circuits or transceivers [4, 5].

A mode-locked device can operate in active, passive or hybrid regime. In the three cases, the longitudinal optical modes are phase-locked and an optical comb is generated. but they are different in nature and the phenomena behind their operation are also distinct, what translates in a dissimilar behavior at all levels [10]. In the passive operation, usually only a saturable absorber (SA) region is used in the device to lock the phase of the optical modes. The passive mode-locked device is completely functional with a DC current signal for the gain section and a DC voltage for the SA region, without the need of a RF reference or any additional external device. Moreover, the phase noise performance in this mode of operation can be extremely good, reaching sub-kHz RF linewidth in the electrical signal associated with the mode-locking repetition rate [11, 12]. Alternatively, under active mode-locking operation, the optical pulses are synchronized to an external RF reference at the mode-locked frequency of the device (or subharmonics). In this case, the pulsed signal can exhibit the phase noise performance of the external reference that could be in the Hz range [13].

It should be noticed that the electrical noise spectra of the beat signal generated under active and passive operation are essentially different. In passive operation, the timing jitter fluctuation appears as a non-stationary process that is unbounded as the spacing between pulses becomes greater, leading to a noise spectra that fits to a curve between Lorentzian and Gaussian depending on the device characteristics. The timing jitter fluctuation associated to active mode-locking is a stationary process, which is externally restored with the RF reference that keep this timing jitter bounded to a value that remains constant independently of the separation between pulses. This is translated to the noise spectrum as a narrow spike (determined by the external reference, i.e. the timing jitter bound) on top of a shape similar to the one that appears in the passive operation [14].

The device used in this work is a Passively Mode-Locked Laser Diode (PMLLD) that has a two contact structure comprised of a SA section of 85  $\mu\text{m}$  length and a gain section of 3915  $\mu\text{m}$  length. The active region contains one InGaAsP/AlGaInAs Quantum Well (QW) emitting at a central wavelength of 1518 nm. Longitudinal confinement of the optical field is achieved by the formation of a 2  $\mu\text{m}$  width ridge waveguide structure. The facet at the absorber end is HR coated (95% reflection) and the output facet is as cleaved [11].

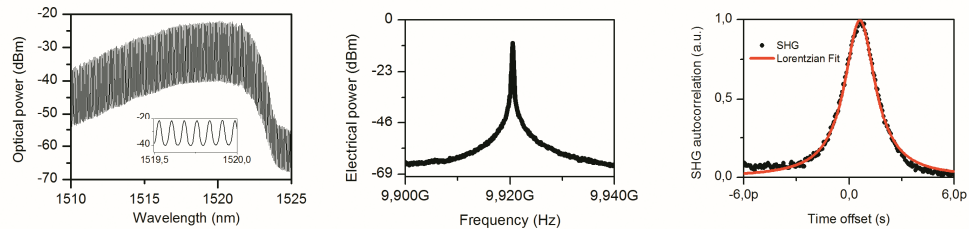


Fig. 1. Optical spectrum (left) and detailed optical spectrum (left inset); electrical spectrum of the fundamental mode-locked frequency (center); and SHG autocorrelation trace with Lorentzian fit (right).

The operation point of the device has been chosen to be within the mode-locking region of the dynamics map of the device. This point corresponds to a current of 115 mA in the gain section and a voltage value of  $-2.6$  V for the SA section. In Fig. 1 the behavior of the device under these conditions is shown. In the leftmost figure the optical spectrum of the device is represented, which exhibits an optical bandwidth of 3 nm ( $\sim 390$  GHz) at 3 dB and 10 nm ( $\sim 1.3$  THz) at 10 dB. The inset details the frequency separation between optical modes ( $\sim 10$  GHz). In Fig. 1 (center) the fundamental beat signal associated with the repetition rate of the device ( $f_{\text{ML}} = 9.92$  GHz) is represented, while the rightmost graph of Fig. 1 contains the Second Harmonic Generation (SHG) autocorrelation trace and its Lorentzian fit. The decorrelated temporal pulses of the device feature a temporal Full Width at Half Maximum (FWHM) of 1 ps, thus having a Time-Bandwidth Product (TBP) equal to 0.39.

### 3. Continuous wave sub-THz photonic synthesis setup

The experimental setup of the CW sub-THz photonic synthesis scheme [9] is shown in Fig. 2. The output of the PMLLD, which is placed in a probe station, is coupled using a lensed fiber that is followed by an optical isolator (ISO1) to prevent back reflections to the device. At this point, 10% of the signal is coupled out for power monitoring purposes (C1), while the rest is optically amplified using an Erbium Doped Fiber Amplifier (EDFA1) after which it is divided in two filtering branches (C2). Each filtering branch allows independent filtering of a selected optical mode of the OFCG through the use of a high Finesse Fabry Perot Tunable fiber Filter (FPTF1-2) that exhibits a 3-dB bandwidth of 6.5 GHz at 1520 nm. An optical isolator (ISO2-3) is also used at each filter output to prevent reflections. Then, both filtering branches are coupled (C3) to obtain a signal containing the two filtered optical modes with a frequency difference equal to the desired CW sub-THz signal. This signal is amplified again with an EDFA (EDFA2) and filtered using a wider bandwidth (130 GHz) tunable optical band pass filter (TF) for ASE suppression in the region outside the bandwidth of interest. After that, a 99:1 optical coupler (C4) allows the monitoring with an Optical Spectrum Analyzer (OSA) of the signal to be photomixed in a fast photodiode (PD, 50 GHz 3-dB bandwidth). Finally, the electrical signal generated in the photodiode with a frequency equal to the difference between the two optical modes is observed in an Electrical Spectrum Analyzer (ESA).

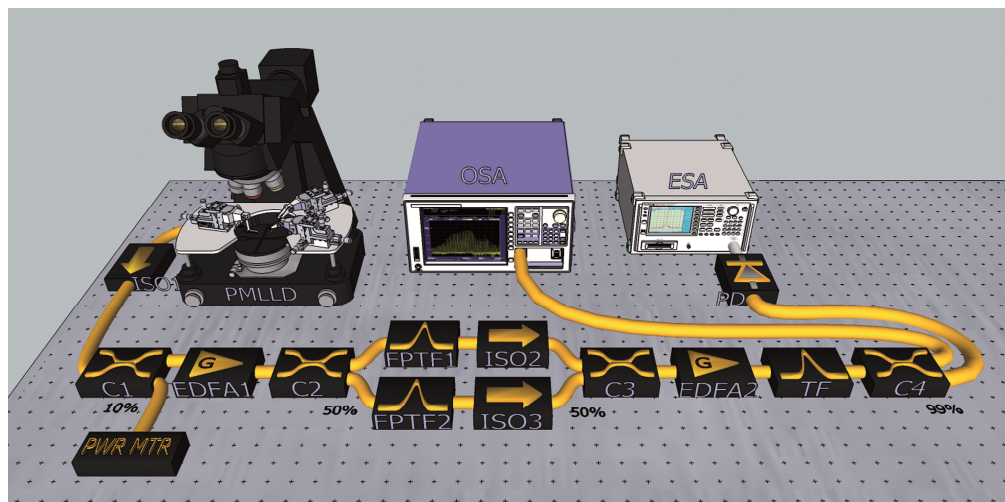


Fig. 2. CW Sub-THz Photonic Synthesis setup. See text for details.

The operation wavelength of the setup around the 1550 nm range allows taking advantage of high performance COTS telecom fiber components. This approach has potential for integration as a Photonic Integrated Circuit (PIC) [4] for a future monolithic implementation of the setup based on the basic building blocks defined on current generic foundry platforms providing active/passive integration [5]. Based on these building blocks, the mode locked source can be implemented in a ring laser structure, while multiple options are available for the optical filters (from rings to array waveguide gratings) and the couplers (from Y-couplers to multimode interference couplers).

## 4. Experimental results

### 4.1 Direct harmonic generation

The most straightforward way of obtaining a mm-wave with an OFCG is the direct harmonic generation, where all the optical modes of the OFCG are photomixed directly generating an electrical comb signal that contains all the harmonics of the fundamental frequency ( $N \cdot f_{ML}$ , being  $N$  the harmonic number). The characteristics of a signal generated this way are well known [13, 14], and for that reason a directly harmonic-generated signal will serve us as a

reference to evaluate the performance of the photonicallly synthesized electrical signals with our setup.

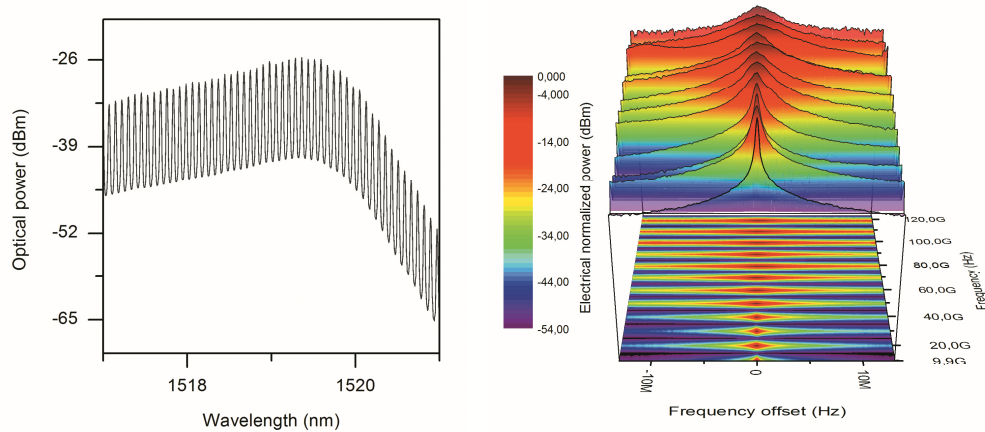


Fig. 3. Direct harmonic generation. Optical spectrum (left) before photomixing, and the generated electrical spectrum after photomixing (right, RBW = 30 kHz), observed at all the harmonics frequencies (fundamental frequency of the PMLL is  $f_{ML} = 9.92$  GHz).

In Fig. 3 (left) the optical spectrum that is photomixed for direct harmonic generation is depicted. This optical spectrum (PMLLD spectrum without mode filtering) generates an electrical signal containing all the harmonics frequencies (Fig. 3, right). The electrical power of the represented electrical spectra is peak normalized. Nevertheless, the reduction in dynamic range given by both the losses of the measurement scheme and the decreasing peak power as the frequency increases can be seen in Fig. 3 (right).

#### 4.2 Photonic synthesis of CW sub-THz signals

The spectra of the photonicallly synthesized signals using the setup from Fig. 2 are shown in Fig. 4. In Fig. 4 (left) it is depicted the selected optical modes employed to synthesize each of the electrical signals represented in Fig. 4 (right). It can be seen that only two optical modes with a frequency separation equal to the desired electrical signal are present in each optical spectrum before detection due to the high selective filtering employed in the setup, which allows to achieve a Side-Supression Ratio (SSR) of  $\sim 11$  dB. These optical spectra generate the corresponding electrical signals appearing in Fig. 4 (right) after photomixing, each of them containing only the frequency represented in the graph, i.e., the required synthesized RF signal. Values for the peak power of the electrical signals of Fig. 4 (corrected for harmonic mixers losses when they are used) as well as the measured noise floor at each synthesized frequency are represented in Fig. 5.

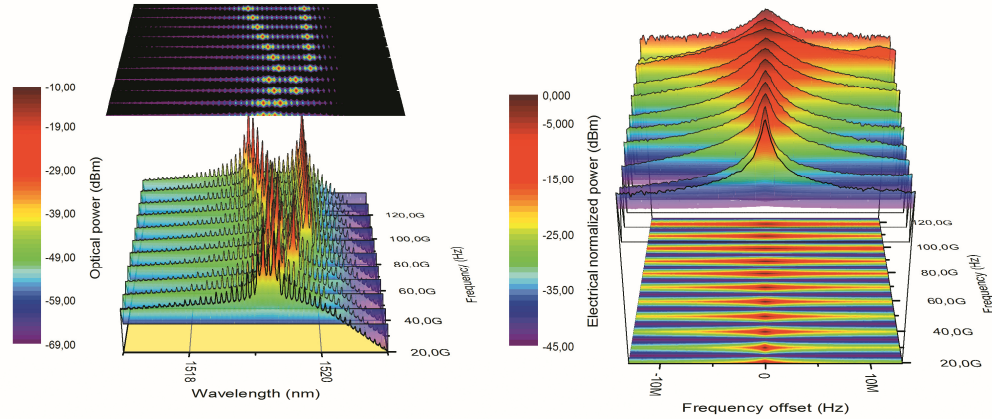


Fig. 4. Photonic synthesis. Optical spectra (left) before photomixing, and the corresponding generated electrical spectra after photomixing (right, RBW = 30 kHz)) for signals between 20 GHz and 119 GHz.

At this point it is important to note that the optical power introduced into the photodiode for the photonic synthesis setup contains only the optical power associated to the two modes separated by the desired frequency. This translates into an optimized use of the optical to electrical conversion compared to direct harmonic generation, where the complete optical spectrum enters the detector to generate an electrical signal that contains power related to all harmonic frequencies. This is important as the maximum output power of the generated electrical signals is limited by the maximum optical input power of the photomixing device, which is low for any photomixing device, but it is better for photodiodes than for photoconductors, especially for improved photodiode structures like Travelling Wave photodiodes (TW PD) or Uni-Travelling-Carrier photodiodes (UTC PD) [15]. So, this scheme allows an optimized use of the available photodetector RF output power.

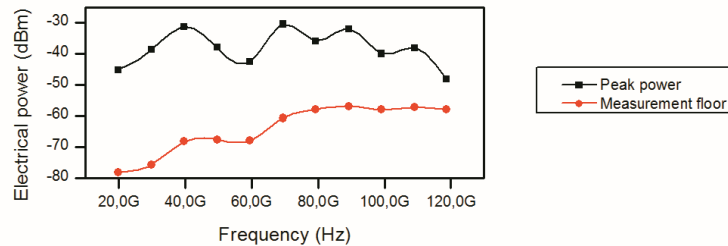


Fig. 5. Electrical peak power (black squares) and measurement floor (red circles) of the electrical signals synthesized with our CW THz photonic synthesis setup.

We should note that the maximum frequency of the synthesized signals is limited both by the bandwidth of the OFCG (1.3 THz of 10-dB bandwidth for our OFCG) and by the photodiode bandwidth. The photodiode used in this experiment has a maximum optical input power of 20 mW and a 3-dB bandwidth of 50 GHz and it is clearly limiting the performance above 100 GHz regardless the high bandwidth available associated to our OFCG. However, state of the art detectors can reach values up to 1 THz in the case of UTC PDs [7] and Travelling Wave Uni-Travelling-Carrier photodiodes (TW-UTC PD) [15]. Hence, the proposed scheme can be readily scaled to synthesize higher RF frequencies. Regarding the frequency resolution of the signals the system can synthesize, there are stabilization techniques, as optical injection, that could offer tuning of the mode-locked frequency up to 270 MHz [16]. This could be the subject for future studies, but it lays beyond the scope of the present work.



### 4.3 Electrical linewidth reduction of the synthesized signals

Once the generation of sub-THz signals using both direct harmonic generation and photonic synthesis is accomplished, we proceed to evaluate the phase noise characteristics of the synthesized signals using as a reference the directly harmonic generated signals. This analysis is done using the 3-dB and 10-dB electrical bandwidth. The losses introduced by the 50 GHz-bandwidth photodiode and the harmonic mixers of the ESA at higher frequencies result in measurements with very limited dynamic range at high frequencies, i.e.  $\sim 10$  dB for 120 GHz, as it can be seen in Fig. 5. This makes the comparison using the Single Side-Band (SSB) noise unfair when comparing across all the required frequency range (20-120 GHz), being this the reason to establish the 3-dB and 10-dB bandwidths as parameters for comparison. The optical amplification stages are the same in both direct harmonic generation (all optical modes) and photonic synthesis (two optical modes) in order to have the same phase noise contribution given by the optical amplifiers, in case it exists. The optical spectrum of the all-modes signal is optically attenuated before photomixing to obtain an electrical signal with a similar power in the frequency of interest for both cases. This allows us to have the same dynamic range in the electrical signals that are compared thus allowing a fair comparison in terms of phase noise and electrical linewidth.

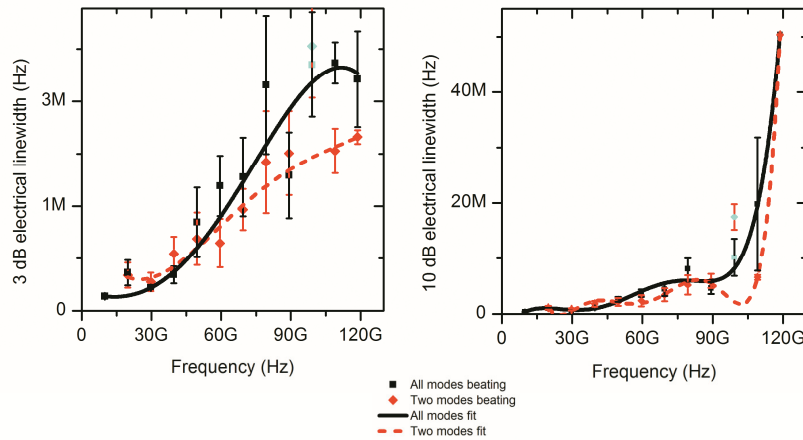


Fig. 6. Comparison between all-modes-beating and two-mode-beating of the 3-dB linewidth (left) and the 10-dB linewidth (right).

The electrical linewidths of the generated electrical signals are represented in Fig. 6. It can be seen for both 3-dB (left) and 10-dB (right) figures that the electrical linewidth of the synthesized signals generated filtering two optical modes is very close to that of the signals generated using all optical modes for frequencies below 50 GHz. For frequencies greater than 50 GHz, the linewidths related with the photonic synthesis using two modes begin to be smaller than those related to direct harmonic generation, and this difference between them seems to increase as the frequency of the synthesized signal gets higher, reaching a 25% reduction for the maximum frequency synthesized (120 GHz) and exhibiting a reduction of 35% for 110 GHz.

The experimental results suggest that under passive mode-locking regime, the photomixing of a greater number of modes may lead to an eventual degradation in the phase noise performance compared to just two-mode beating because of the unbounded behavior of the timing jitter fluctuations under passive operation which follow a random walk trend [14], and whose addition could worsen the total timing jitter and thus the phase noise. This is just opposite to the expected in the active case, where the contribution of more modes should improve the phase noise of the generated signals [17], as the timing jitter fluctuations are always bounded by an external reference [14].

The trend of this reduction is not followed by the signals generated at 99 GHz, what can be caused by an anomalous behavior of the device at this point, generating an additional spurious signal separated  $\sim 1$  MHz, as represented in the right graphs of Fig. 3 and Fig. 4. It must be noticed also that the comparison for the 119 GHz signals is significantly affected by the dynamic range of the measurement scheme at this frequency ( $\sim 10$  dB, see Fig. 5) resulting in a broader 10-dB linewidth for the synthesized signal that does not follow the trend observed before this point.

Finally, it is important to remark that the amplitude jitter associated to possible drifts of the central frequency of the FPTFs will have no significant contribution to the SSB noise, even in the case of strong amplitude fluctuations. Under passive mode-locking operation, the SSB noise is expected to be basically caused only by the timing jitter as demonstrated in [14]. This can be considered as an advantage of our setup over more complex systems that rely on OPLL for sub-THz signal generation where phase instabilities in the loop are directly translated to timing jitter and therefore to SSB noise.

## 5. Conclusions

A compact and straightforward setup for Continuous Wave (CW) sub-THz photonic synthesis has been implemented and experimentally studied. The scheme proposed is based on the selective filtering of longitudinal optical modes from a Passively Mode-Locked Laser Diode (PMLLD), which acts as an Optical Frequency Comb Generator (OFCG), and their photomixing in a fast photodiode with the objective of studying the phase noise characteristics of the generated signal. In order to do this, the synthesized signal has been compared to the signal generated after the mixing of all the optical modes of the OFCG, whose characteristics are well known. This scheme does not need an Optical Phase Lock Loop (OPLL), as it is based on the use of a PMLLD as OFCG, which in addition does not need any RF signal or phase modulation. Hence, this scheme is cost-effective and potentially integrated as a PIC based on the current basic building blocks that are made available on generic foundry platforms.

Photonic synthesis of CW electrical signals up to 120 GHz using a 50 GHz photodiode has been experimentally achieved using this scheme. The phase noise performance it exhibits, based on the evaluation of the 3-dB and 10-dB electrical linewidths, has been analyzed for the synthesized signals taking as a reference the electrical signals obtained with direct harmonic generation. No significant differences have been observed below 50 GHz, but from this frequency onwards, it can be appreciated a linewidth reduction trend that becomes greater as the frequency increases, reaching reductions of 35% at 110 GHz and 25% at 120 GHz.

The reported phase noise improvement of CW sub-THz signals synthesized with this setup along with its integration potential, cost and bandwidth capabilities make it a promising candidate to the development of an integrated and high performance local oscillator in the sub-THz range.

## Acknowledgments

Work supported by the Spanish Ministry of Science and Technology through the project TEC2009-14525-C02-02 and by the European Commission FP7 iPHOS Project. The work by A.R. Criado has been supported by the Spanish Ministry of Science and Technology under the FPI Program, Grant# BES2010-030290.